Published in final edited form as:
J Neuroimmunol. 2011 March ; 232(1-2): 26–34. doi:10.1016/j.jneuroim.2010.09.029.

STAT6$^{-/-}$ mice exhibit decreased cells with alternatively activated macrophage phenotypes and enhanced disease severity in murine neurocysticercosis

Bibhuti B. Mishra, **Uma Mahesh Gundra**, and **Judy M. Teale***
Department of Biology, South Texas Center for Emerging Infectious Diseases, University of Texas at San Antonio, One UTSA Circle, San Antonio, Texas 78249-1644.

Abstract

In this study, using a murine model for neurocysticercosis, macrophage phenotypes and their functions were examined. *Mesocestoides corti* infection in the central nervous system (CNS) induced expression of markers associated with alternatively activated macrophages (AAMs) and a scarcity of iNOS, a classically activated macrophage marker. The infection in STAT6$^{-/-}$ mice resulted in significantly reduced accumulation of AAMs as well as enhanced susceptibility to infection coinciding with increased parasite burden and greater neuropathology. These results demonstrate that macrophages in the helminth infected CNS are largely of AAM phenotypes, particularly as the infection progresses, and that STAT6 dependent responses, possibly involving AAMs, are essential for controlling neurocysticercosis.

Keywords

Neurocysticercosis; helminth; alternatively activated macrophages; CNS; STAT6

Introduction

Neurocysticercosis (NCC) is the most common parasitic disease worldwide which affects the central nervous system (CNS). The disease occurs as a result of infection of the brain with the larval stage of the tape worm parasite *Taenia solium* (*T. solium*) (Davis and Kornfeld, 1991; Nash et al., 2006; Sciutto et al., 2007; Terrazas, 2008; White, 2000). Interestingly, in NCC humans remain asymptomatic for long periods of time (months to years). The infection becomes apparent upon degeneration of larvae caused by either therapeutic treatment or normal attrition resulting in severe headaches, epilepsy, intracranial hypertension, focal deficit, and/or cognitive impairment (Nash et al., 2006). These disease symptoms are frequently associated with an intense immune response induced by the dead parasite (Correa et al., 1985; Grewal et al., 2000). The precise immune response induced in

*Send correspondence and reprint requests to: Judy M. Teale, Ph.D., Department of Biology, The University of Texas at San Antonio, One UTSA Circle, San Antonio, TX 78249-1644; Tel: (210) 458-7024; Fax: (210) 458-7025; judy.teale@utsa.edu.

Disclosures
The authors have no financial conflict of interest.

the context of the CNS during NCC has been addressed mainly via analysis of helper T cell (Th) responses. This response is characterized by an overt Th1 phenotype (Restrepo et al., 1998), or a mixed Th1, Th2, and Th3 phenotype depending upon the absence or presence of granuloma formation and the stage of the granulomatous response (Restrepo et al., 2001). However, evidence regarding the appropriate immune responses required in controlling the infection or the clinical outcome of NCC is unknown.

The ability to elicit an immune response to infections is orchestrated, in large part, by specialized innate cell types such as macrophages. However, less attention has been paid to identifying the role of macrophages in the CNS microenvironment during NCC. In this context, macrophages activated during Th1-type responses, such as elicited by bacterial and viral infections, exhibit an inflammatory phenotype and produce proinflammatory cytokines, oxygen and nitrogen radicals (Nathan and Shiloh, 2000). In contrast, macrophages during helminth parasitic infection have an alternatively activated phenotype (Kreider et al., 2007). These AAMs exhibit an anti-inflammatory and a protective role in conjunction with the induced Th2- type response (Kreider et al., 2007; Noel et al., 2004). AAMs are thought to be involved in tissue repair and remodeling at the site of injury (Gordon, 2003; Mosser, 2003). This is of considerable importance during helminth infection as large metazoan parasites can cause extensive damage as they pass through tissue, releasing proteolytic enzymes that damage cells and tissue (Kreider et al., 2007). At the same time, AAMs largely fail to produce nitric oxide (NO) due to their induction of arginase (Gordon, 2003). This has led to the speculation that impairment of microbial killing functions of these cells can increase host susceptibility to infection. Correlatively, several studies have demonstrated that STAT6 knockout (KO) mice, which typically exhibit a defect in AAM associated responses as well as upregulated classically activated macrophage (CAM) associated responses, display enhanced anti-microbial immunity in a variety of parasitic disease models (Reyes and Terrazas, 2007). This suggests a role for STAT6 and AAMs in facilitating the establishment of a chronic infection (Reyes and Terrazas, 2007). In a contrasting situation, STAT6 associated responses are thought to be required for the expulsion of helminth parasites (Finkelman et al., 2004; Gause et al., 2003; Urban et al., 1998; Voehringer et al., 2007). Thus, an important question is whether CNS helminth infections such as in NCC induce AAMs in the brain microenvironment.

In an experimental murine model for NCC developed in our laboratory (Cardona et al., 1999), mice intracranially (i.c.) inoculated with *Mesocestoides corti* (*M. corti*) metacestodes display an inflammatory CNS immune response which is similar in nature to human NCC (Cardona et al., 2003; Cardona et al., 1999; Cardona and Teale, 2002; Mishra et al., 2009). In this study, analysis of the expression of AAM associated molecules and iNOS in the CNS of *M. corti* infected mice was performed. Additionally, the effect of the absence of AAM development/accumulation on the subsequent susceptibility and immunopathology in infected STAT6$^{-/-}$ mice was compared with WT mice. The evidence indicates that the absence of STAT6 mediated responses results in increased disease severity possibly through the lack of AAMs.

Materials and Methods

Mice

Female STAT6$^{-/-}$ on C57BL/6 background, wildtype (WT) C57BL/6 mice were obtained from the Jackson Laboratory (Bar Harbor, Maine). Female BALB/c mice were used in this study for parasite maintenance and were obtained from the National Cancer Institute animal program (Bethesda, MD). All animal experiments were conducted under the guidelines of the IACUC, UTSA, University of Texas System, the U.S. Department of Agriculture and the National Institutes of Health.

Antibodies

Phycoerythrin (PE)-conjugated anti-mouse CD11b (Mac-1), biotinylated anti-mouse CD11b, biotinylated anti-mouse CD11c and anti-mouse iNOS antibodies were purchased from BD PharMingen (San Diego, CA). AAMs in the brain were detected by using purified anti-mouse YM1 (ECF-L) (R&D Systems, USA), anti-mouse Fizz1 (RELMα) (Abcam, Cambridge, MA) or anti-mouse arginase 1 (ARG-1) (Santa Cruz Biotechnology, CA, USA). Purified anti-mouse mannose receptor 1 (MR1) and anti-mouse macrophage galactose-type C-type lectins (MGL1/2) were purchased from R&D System. For indirect immunofluoresence, appropriate fluorescent conjugated secondary antibodies (Jackson Immuno Research Laboratories, West Grove, PA) were used. Biotinylated primary antibodies were detected using Alexa Fluor 488-labeled streptavidin (Molecular Probes, USA).

Murine model of neurocysticercosis

In this study we used a mouse model of NCC developed in our laboratory (Cardona et al., 1999; Cardona and Teale, 2002). *M. corti* tetrathyridia (immature stage) were maintained by serial intraperitoneal (i.p.) inoculation of 8- to 12 wk-old female BALB/c mice. Tetrathyridia were aseptically harvested, and murine NCC was induced by i.c. injection of 50 μl of HBSS containing approximately 40 organisms into 5 wk old mice under short-term anesthesia using a 50 μl mixture of ketamine HCL and xylazine (30 mg/ml ketamine and 4 mg/ml xylazine) in phosphate buffered saline (PBS) intramuscularly, as described previously (Cardona et al., 1999). Mock infected control mice were similarly injected with 50 μl sterile HBSS alone. At indicated times post-inoculation, anaesthetized animals were perfused through the left ventricle with 10 ml cold PBS, and brains were harvested to analyze parasite burden and various immune parameters.

RNA isolation and Real-Time PCR analysis

To determine the gene expression of YM1, Fizz1, ARG-1 and iNOS in murine NCC, brains were removed from infected and vehicle control mice at 1 wk and 2 wk post infection (p.i.). Animals were perfused with PBS prior to sacrifice to avoid RNA contamination from blood cells. Brains were immediately removed after perfusion. Total RNA was extracted using Trizol reagent (Invitrogen) according to manufacturers' instructions, and cDNA was prepared from 1 μg total RNA using the High Capacity cDNA Archive Kit (Applied Biosystems). The cDNA derived from brains of mock and parasite-infected mice were loaded onto microfluidic cards preloaded with fluorogenic probes and primers for custom-designed Taq-Man Low Density Arrays (Applied Biosystems, CA, USA) for AAM and CAM markers and housekeeping genes β-actin, ribosomal 18S, and GAPDH (glyceraldehyde 3-phosphate dehydrogenase). These cards were then loaded for thermal cycling on an ABI Prism 7900 HT Sequence Detection System (Applied Biosystems). Analyses of gene expression were determined using the ABI Prism 7900 Sequence Detection System software (Applied Biosystems). The target expression levels were normalized to levels of the house keeping genes 18S, β-actin and GAPDH in the same sample. Expression of each specific gene in infected samples was determined as fold change over that in control samples as calculated by using the formula $2^{-(\Delta\Delta Ct)}$.

Histology and immunofluorescence staining

The brains were immediately removed from perfused animals, embedded in O.C.T. resin (optimal cutting temperature), and snap frozen. Serial horizontal cryosections, 10 μm in thickness, were placed on silane prep slides (Sigma-Aldrich, St. Louis, MO). One in every four slides was fixed in formalin for 12 min at room temperature and stained with hematoxylin and eosin (H&E), as described previously (Mishra et al., 2009). The remainder

of the slides were air-dried overnight and fixed in fresh acetone for 20s at room temperature. Acetone-fixed sections were wrapped in aluminum foil and stored at −80°C or processed immediately for *in situ* immunofluorescence (IF) microscopy analysis as previously described (Alvarez and Teale, 2007a; Alvarez and Teale, 2007b; Cardona et al., 2003; Mishra et al., 2006).

Quantification of expression levels of immune mediators

Sections of brains from mock-infected and NCC mice (WT and STAT6$^{-/-}$) were stained with anti-YM1, anti-ARG-1, ant-Fizz1, anti-iNOS, anti-MR1, and anti-MGL1/2 antibodies followed by labeled secondary antibodies to determine potential differences in infection induced expression levels between WT and STAT6$^{-/-}$ mice. Some brain sections were additionally stained with antibodies to the macrophage marker CD11b to assess co-localization with YM1, Fizz1, ARG-1, MR1, MGL1/2, and iNOS. Protein level expression of these molecules was determined by capturing images at 20X magnification in the brain of mock infected and NCC animals using identical camera settings so that the number and intensity of pixels would reflect differences in protein expression (Mishra et al., 2008; Mishra et al., 2009). The area (number of pixels) and fluorescence intensity (average intensity of pixels) of the staining was measured from ten images captured in brain areas containing infiltrating immune cells. This was done using the imaging software IP lab 4.0 (BD Biosciences Bioimaging, Rockville MD). The relative expression of YM1, Fizz1, ARG-1, iNOS, MR1, and MGL1/2 was calculated by multiplying the number of pixels (area) by the average intensity of pixels.

Statistical analysis

Statistical analysis was performed with a Student's *t*-test using SIGMA PLOT 8.0 (Systat Software, San Jose, CA). A p value less than 0.05 was considered to be statistically significant. Statistical differences in mortality of parasite-infected WT and STAT6$^{-/-}$ mice were analyzed using Kaplan Meier survival analysis.

Results

Expression of AAM associated markers in the CNS after *M. corti* infection

Quantitative real-time PCR analysis was performed to determine the expression profile of AAM associated marker molecules YM1, Fizz1, ARG-1, and CAM associated molecule iNOS in mock control and parasite-infected brains. Upon infection with *M. corti*, the CNS displayed upregulation of transcript level expression of AAM associated molecules by five hundred to several thousand folds over those in mock animals at both 1wk and 2wk p.i. (Fig. 1). In contrast, there was only a moderate increase in the mRNA level of the CAM associated molecule iNOS compared to the expression of AAM related molecules (Fig. 1).

To examine the expression of these molecules at the protein level, *in-situ* IF microscopy was used. In uninfected animals, the AAM related molecules YM1, Fizz1, and ARG-1 were undetected (Fig. 2 A1, B1, and C1). Upon infection, YM1, Fizz1, and ARG-1 were found to be abundantly expressed in the CNS at 1 wk p.i. (Fig. 2 A2, B2, and C2) and 3 wk p.i. (Fig. 2 A3, B3, and C3). These AAM associated molecules appeared to be extracellular as well as cytosolic (Fig. 2 A2', A3', C2', and C3'). In contrast, iNOS was scarcely detected in both mock (Fig. 2D1) and parasite-infected brains at these times p.i. (Fig. 2 D2 and D3). Quantification of the protein level expression of these molecules in terms of mean pixel intensity in mock or parasite-infected brain sections confirmed that parasite infection increased the expression of AAM associated molecules in the CNS by several thousand fold compared to mock controls, but there was no substantial difference in protein expression of iNOS (Fig. 4).

STAT6 deficiency downregulates the expression of AAM associated molecules in *M. corti* infected brains

As reported previously, STAT6 dependent mechanisms play an important role in the development of AAMs (Kreider et al., 2007; Martinez et al., 2009). Therefore, we determined the expression of AAM associated molecules in parasite-infected brain cryosections of WT and STAT6$^{-/-}$ mice by IF staining (Fig. 3). In mock-infected brains of both WT and STAT6$^{-/-}$ mice, YM1, Fizz1, and ARG-1 were scarcely detected (Fig. 2 A1, B1, C1 and data not shown). Upon infection, the WT mice displayed a progressive increase in the levels of these molecules as measured both by intensity of staining and the number of positive cells. At 1 wk (data not shown) and 2 wk p.i. a majority of the infiltrating macrophages (CD11b+ cells) were detected positive for YM1 (Fig. 3A1), Fizz1 (Fig. 3B1), and ARG-1 (Fig. 3C1). In contrast, STAT6$^{-/-}$ mice displayed minimal expression of these AAM markers both by intensity of staining and the number of positive cells at 1 wk (data not shown) and 2 wk p.i. (Fig. 3 A2, B2, and C2). Quantification of the mean pixel intensity of YM1, Fizz1 and ARG-1 staining confirmed that these AAM markers were detected at significantly lower levels at both 1 wk and 2 wk p.i. in parasite-infected STAT6$^{-/-}$ mice compared to WT infected mice (Fig. 4 A and B). The accumulation of AAMs in the parasite-infected WT and STAT6$^{-/-}$ brains was further analyzed by double IF staining of CD11b and cell surface receptors that are specifically expressed by AAMs: MGL1/2 (Raes et al., 2005) and MR1 (Gordon, 2003; Stein et al., 1992). Similar to the expression of other AAM associated molecules, MR1 and MGL1/2 were undetected at the protein level in the mock control WT and STAT6$^{-/-}$ brains (data not shown). Upon parasite infection, the WT mice exhibited an accumulation of large numbers of macrophages / microglia (CD11b+ cells) expressing MR1 and MGL1/2 at all p.i. times analyzed (Fig. 3 D1 and E1). In contrast, although the parasite-infected STAT6$^{-/-}$ mice exhibited a similar accumulation of CD11b+ cells in the CNS, few CD11b+ cells displayed positive staining for MR1 and MGL1/2 (Fig. 3 D2 and E2). Moreover, measurement of mean pixel intensity confirmed that expression of MR1 and MGL1/2 was significantly lower in parasite-infected STAT6$^{-/-}$ mice brain as compared to the WT controls (Fig. 4 A and B).

Because of its higher affinity for arginine, upregulated ARG-1 in AAMs typically out-competes iNOS which metabolizes arginine in CAMs (Modolell et al., 1995; Munder et al., 1998). Therefore, upregulated ARG-1 expression in AAMs which is indicative of AAM induction is also indicative of suppression of CAM differentiation (Kreider et al., 2007). IF microscopic analysis indicated that WT NCC mice exhibited low basal to undetected levels of iNOS expression (Fig. 3F1). In contrast, infected STAT6$^{-/-}$ mice displayed a progressive increase in the levels of iNOS protein as measured both by intensity of staining and number of positive cells (Fig. 3F2). Measurement of mean pixel intensity confirmed that iNOS was expressed at significantly higher level in parasite-infected STAT6$^{-/-}$ mice brain than their WT counterparts (Fig. 4). Taken together, the results suggest that STAT6 associated signaling dictates the activation phenotypes in the CNS to the AAM phenotype during NCC.

STAT6$^{-/-}$ mice are more susceptible to parasite infection in murine NCC

Since tissue restoration and repair is one of the well-defined regulatory properties of AAMs (Gordon, 2003; Kreider et al., 2007; Martinez et al., 2009), we investigated whether the lack of AAMs in STAT6$^{-/-}$ mice affected disease outcome. To this end, disease severity was compared between WT and STAT6$^{-/-}$ mice infected i.c. with *M. corti*. As has been reported previously (Cardona et al., 1999; Cardona and Teale, 2002; Mishra et al., 2009), infected WT mice displayed typical neurological signs including abnormal vestibular function, tilted head, mice walking in circles around the cage, and morbidity, after 1 wk p.i. The STAT6$^{-/-}$ mice exhibited more severe neurological signs during the first 2 wks p.i. Importantly, by 15 days p.i., 100% of *M. corti*-infected STAT6$^{-/-}$ mice (10 of 10) succumbed to the infection,

whereas, only 33% of WT mice (5 of 15) had succumbed to the infection by this p.i. time (Fig. 5, $p<0.005$). Thus, deficiency of STAT6 signaling in mice resulted in increased disease severity and mortality during murine NCC.

STAT6$^{-/-}$ mice exhibit increased parasite load in brain

To examine whether increased disease severity in STAT6 deficient mice was associated with a lack of effective clearance of parasites, serial horizontal sections of infected WT and STAT6$^{-/-}$ brains were stained with H&E, and the number of *M. corti* metacestodes was determined by microscopic analysis. Mice deficient in STAT6 appeared less able to control parasite growth, as the brains of these mice exhibited increased numbers of parasites as compared to the infected brains of WT mice (Fig. 6). The STAT6$^{-/-}$ mice displayed an elevated CNS parasite burden after 1 wk p.i. (Fig. 6) that was significantly increased by ~ 2.5-fold over the number of parasites in corresponding WT mice at 2 wk p.i. (Fig. 6). At both 1 wk and 2 wk p.i., most of the *M. corti* parasites were localized to the brain parenchyma in STAT6$^{-/-}$ mice (Fig. 6). These analyses demonstrated that STAT6 dependent responses may be critical regulators of controlling parasite growth and invasiveness in the CNS during NCC.

STAT6$^{-/-}$ mice display increased CNS pathology after *M. corti* infection

The increased number of parasites in brains of STAT6$^{-/-}$ mice may cause increased pathology due to either the mechanical disruption of brain tissue or the metabolic activity of parasites. H&E staining was performed to determine immunopathological changes in the WT and STAT6$^{-/-}$ mice (Fig. 7). Fig. 7, A1 and A2, depict normal brain tissue morphology in WT and STAT6$^{-/-}$ control animals i.c. inoculated with HBSS. In contrast, CNS infection in WT and STAT6$^{-/-}$ mice resulted in strong inflammatory responses characterized by the presence of a large number of infiltrating immune cells which were predominantly monocytic in nature (Fig. 7 B1 and B2; star). However, in the parasite-infected WT mice, a large proportion of parenchymal parasites (P) was surrounded by infiltrating leukocytes (Fig. 7C1), whereas the STAT6$^{-/-}$ mice displayed scarce numbers of infiltrating immune cells around parenchymal parasites (Fig. 7C2). These immunopathological events were evident at both 1 wk and 2 wk p.i., although more so at 2 wk p.i. Next, the changes in nervous tissue integrity in WT and STAT6$^{-/-}$ mice was determined in the H&E stained brain cryosections by analyzing the presence (and size) of microglial nodule formation which reflects engulfment of degenerating neurons and necrotic brain tissue by glia cells. In STAT6$^{-/-}$ infected mice, primary and secondary microglial nodule formation were detected by 1 wk p.i. (Fig. 7D2), but not in WT infected mice (Fig. 7D1). Together, the data suggest that absence of STAT6 dependent responses leads to increased CNS pathology during murine NCC.

Discussion

Macrophages play an indispensable role in the defense against pathogens and in the maintenance of tissue homeostasis. They comprise a heterogeneous population with inflammatory (classical) or reparative (alternative) properties which can be identified based on their phenotypic characteristics (Gordon, 2003; Joshi et al., 2008; Lumeng et al., 2007; Martinez et al., 2006; Martinez et al., 2009; Umemura et al., 2008). The CAMs exhibit potent antimicrobial properties and promote Th1 responses while AAMs support Th2-associated effector functions. AAMs also play a role in the resolution of inflammation through their high endocytic clearance capacities and the synthesis of trophic factors (Mantovani et al., 2007). Although macrophages represent the predominant infiltrating immune cell population in both human and murine NCC (Alvarez et al., 2010), their phenotypic and functional characteristics in the brain are largely unknown. This study shows

that many of the macrophages/ microglia cells in the brain during murine NCC are of AAM phenotypes.

STAT6 associated signaling has been the best characterized regulatory pathway shown to participate in AAM development (Martinez et al., 2009). STAT6 is a primary signaling molecule that interacts with the host membrane receptor IL-4Rα, which, upon binding to IL-4 and IL-13, activates an intracellular signaling cascade involving the Janus kinase pathway (Keegan et al., 1995; Leonard and O'Shea, 1998; Moy et al., 2001; Nelms et al., 1999; Obiri et al., 1995; Obiri et al., 1997). This culminates in the phosphorylation of STAT6 which dimerizes and binds to promoters of several genes involved in AAM-associated acquired immunity (Chomarat and Banchereau, 1998). AAMs termed M2a (induced by IL-4/IL-13) (Munder et al., 1998; Pauleau et al., 2004) and M2c (induced by IL-10) (Mantovani et al., 2004), typically display the arginase pathway activation and are thought to play an important role in regulating immune responses to helminths. Indeed, *M. corti* i.p. infected IL-$4^{-/-}$ mice display significantly lower expression of YM1 and Fizz1, although ARG-1 expression as well as activation of CAMs in the liver was unchanged (O'Connell et al., 2009). However, in the CNS during *M. corti* infection larger amounts of IFN-γ and TNF-α are detected, and importantly IL-4, IL-13 and IL-10 are detected in relatively low/scarce amounts (Cardona et al., 1999). This suggests a possible involvement of additional host and/or pathogen derived molecules in AAM development during murine NCC. Indeed, emerging evidence indicates that in addition to host-derived factors, AAMs can also be induced by pathogen-derived signals (Mantovani et al., 2005; Martinez et al., 2008; Mosser, 2003). In this regard, a recent study showed that schistosomal LNFPIII glycan antigens induced expression of AAM associated markers ARG-1 and YM-1 in macrophages of IL-4Rα$^{-/-}$ mice, suggesting existence of an innate pathway for initiating AAMs independent of IL-4 or IL-13 (Atochina et al., 2008). Furthermore, in a study comparing responses during *Nippostrongylus brasiliensis* infection in WT and severe-combined immune deficient (SCID) mice, both strains of mice transcribed a similar level of the AAM associated genes: YM1, Fizz1, and ARG-1 during the innate immune phase of infection (Reece et al., 2006). In light of the low levels of Th2 cytokines detected in our model coupled with the fact that AAMs expressing Fizz1 and ARG-1 suppress Th2 responses (Pesce et al., 2009a; Pesce et al., 2009b) collectively suggest that innate immune responses in the CNS to *M. corti* may be involved in the development of AAMs during NCC. We propose that the abundant release/secretion of glycans observed in CNS infections with cestodes like Mesocestoides and Taenia (Alvarez et al., 2008) may be responsible for the induction of AAMs in a Th2-axis independent manner. The mouse model of NCC thus provides a unique opportunity to identify the innate immune mechanisms involved in recognition of parasite glycans by host pattern recognition receptors (PRRs) and subsequent development of AAMs. This is a major focus of the current research in our laboratory.

The present study demonstrates a key role for STAT6 as a critical regulator in CNS immunity during experimental NCC, as a deficiency in STAT6 led to greater morbidity and mortality during *M. corti* infection in the CNS. Since STAT$6^{-/-}$ mice also display higher numbers of parasites in the CNS parenchyma, it is likely that STAT6 associated responses play a role in limiting parasite growth in brain parenchyma. This is consistent with studies involving other parasite infections where Th2 dependent AAM associated responses directly mediate parasite clearance and host protection (Anthony et al., 2006; Finkelman et al., 2004; Gause et al., 2003; O'Connell et al., 2009; Reyes and Terrazas, 2007; Voehringer et al., 2007). Although a direct role of STAT6 dependent AAM associated responses was not established in the present study, the enhanced disease severity of STAT$6^{-/-}$ NCC mice correlated with decreased numbers of AAMs in the CNS as compared to WT mice. This indicates a possible protective role of these cells in NCC. Particularly, STAT6 dependent AAM associated anti-inflammatory/immune suppressive events (Harn et al., 2009; Kreider

et al., 2007; Reyes and Terrazas, 2007) may be important to reduce pathologic inflammatory responses in the brain during murine NCC. This is supported by the fact that frequently in CNS diseases, sustained inflammation is the cause of tissue damage and associated pathology (Chavarria and Alcocer-Varela, 2004). Within this context, *M. corti* infected STAT6$^{-/-}$ mice display an upregulation of the Th1 effector molecule iNOS and NO is known to be particularly deleterious in the CNS and likely to be highly regulated (Brosnan et al., 1994; Chao et al., 1992; Lehnardt et al., 2006). In this regard, despite the presence of a predominant inflammatory response in the CNS of WT NCC mice (Cardona et al., 1999; Mishra et al., 2009), particularly at the early stages of infection, our results indicate that iNOS is expressed at relatively low levels at the time points tested. The increasing expression of AAM associated molecules during the course of infection, including at 6wk p.i. (data not shown), likely helps to control the expression of such inflammatory mediators. Macrophages typically display remarkable plasticity and can change their properties depending upon the surrounding milieu (Mosser and Edwards, 2008), presumably altering the characteristics/proportion of CAMs and AAMs during the course of NCC. Nonetheless, the results from this study strongly suggest that the scarcity of AAM associated protective functions in the CNS likely contributes to the increased disease severity in STAT6$^{-/-}$ NCC mice. Another likely contributor is the higher worm burden in brain parenchyma with a lack of surrounding infiltrating immune cells, particularly AAMs, in STAT6$^{-/-}$ NCC mice, which would lead to direct exposure of CNS tissue to damaging molecules released by the parasite.

A deficiency of AAM associated responses in STAT6$^{-/-}$ NCC mice can lead to a defect in tissue repairing/restoration mechanisms as these cells have been shown to contribute to fibrosis and repair at the site of injury (Kigerl et al., 2009; Kreider et al., 2007). This is of considerable importance during helminth infection as large metazoan parasites such as *M. corti* and *T. solium* can cause extensive damage as they pass through tissue, releasing proteolytic enzymes that damage cells and tissue (van Riet et al., 2007). In this light, increasing evidence suggests that in diseases involving helminth parasites, development of AAMs is a hallmark of infection, with tissue repair as their primary function (Harn et al., 2009; Martin and Leibovich, 2005; Martinez et al., 2009). This hypothesis has been driven by the knowledge that high arginase activity in AAMs contributes to production of proline, which is an important precursor of collagen and polyamines that are involved in cell proliferation and fibrosis (Hesse et al., 2001). Moreover, AAMs exhibit increased expression of host lectins like MR1 and MGL1 that can directly participate in tissue restorative mechanisms (Gordon, 2003). For example, MR1 binds to late-stage apoptotic and necrotic cells and facilitates removal of dying cells without causing bystander damage or inflammatory responses (Nauta et al., 2003). Additionally, MGL1 has been demonstrated to play a role in tissue formation and restoration during inflammation induced pathology (Saba et al., 2009; Sato et al., 2005). However, it is unknown whether a similar mechanism plays a role in limiting tissue pathology in STAT6$^{-/-}$ NCC mice that lack the expression of MR1 and MGL1/2. Studies are currently underway in our laboratory to define MR1 and MGL1 functions in AAMs, particularly their role in tissue restoration/remodeling during murine NCC.

The present study demonstrates that STAT6 functions in promoting AAM associated responses in the CNS microenvironment. The data strongly support a protective role for STAT6 associated signaling in controlling the disease severity of murine NCC.

Acknowledgments

Supported by awards NS 35974, AI 59703 and P01 AI 057986 from the National Institutes of Health

References

Alvarez JI, Mishra BB, Gundra UM, Mishra PK, Teale JM. Mesocestoides corti intracranial infection as a murine model for neurocysticercosis. Parasitology. 2010; 137:359–372. [PubMed: 20109250]

Alvarez JI, Rivera J, Teale JM. Differential release and phagocytosis of tegument glycoconjugates in neurocysticercosis: implications for immune evasion strategies. PLoS Negl Trop Dis. 2008; 2:e218. [PubMed: 18398489]

Alvarez JI, Teale JM. Differential changes in junctional complex proteins suggest the ependymal lining as the main source of leukocyte infiltration into ventricles in murine neurocysticercosis. J Neuroimmunol. 2007a; 187:102–113. [PubMed: 17597230]

Alvarez JI, Teale JM. Evidence for differential changes of junctional complex proteins in murine neurocysticercosis dependent upon CNS vasculature. Brain Res. 2007b; 1169:98–111. [PubMed: 17686468]

Anthony RM, Urban JF Jr, Alem F, Hamed HA, Rozo CT, Boucher JL, Van Rooijen N, Gause WC. Memory T(H)2 cells induce alternatively activated macrophages to mediate protection against nematode parasites. Nat Med. 2006; 12:955–960. [PubMed: 16892038]

Atochina O, Da'dara AA, Walker M, Harn DA. The immunomodulatory glycan LNFPIII initiates alternative activation of murine macrophages in vivo. Immunology. 2008; 125:111–121. [PubMed: 18373667]

Brosnan CF, Battistini L, Raine CS, Dickson DW, Casadevall A, Lee SC. Reactive nitrogen intermediates in human neuropathology: an overview. Dev Neurosci. 1994; 16:152–161. [PubMed: 7535680]

Cardona AE, Gonzalez PA, Teale JM. CC chemokines mediate leukocyte trafficking into the central nervous system during murine neurocysticercosis: role of gamma delta T cells in amplification of the host immune response. Infect Immun. 2003; 71:2634–2642. [PubMed: 12704138]

Cardona AE, Restrepo BI, Jaramillo JM, Teale JM. Development of an animal model for neurocysticercosis: immune response in the central nervous system is characterized by a predominance of gamma delta T cells. J Immunol. 1999; 162:995–1002. [PubMed: 9916725]

Cardona AE, Teale JM. Gamma/delta T cell-deficient mice exhibit reduced disease severity and decreased inflammatory response in the brain in murine neurocysticercosis. J Immunol. 2002; 169:3163–3171. [PubMed: 12218134]

Chao CC, Hu S, Molitor TW, Shaskan EG, Peterson PK. Activated microglia mediate neuronal cell injury via a nitric oxide mechanism. J Immunol. 1992; 149:2736–2741. [PubMed: 1383325]

Chavarria A, Alcocer-Varela J. Is damage in central nervous system due to inflammation? Autoimmun Rev. 2004; 3:251–260. [PubMed: 15246020]

Chomarat P, Banchereau J. Interleukin-4 and interleukin-13: their similarities and discrepancies. Int Rev Immunol. 1998; 17:1–52. [PubMed: 9914942]

Correa D, Dalma D, Espinoza B, Plancarte A, Rabiela MT, Madrazo I, Gorodezky C, Flisser A. Heterogeneity of humoral immune components in human cysticercosis. J Parasitol. 1985; 71:535–541. [PubMed: 3903094]

Davis LE, Kornfeld M. Neurocysticercosis: neurologic, pathogenic, diagnostic and therapeutic aspects. Eur Neurol. 1991; 31:229–240. [PubMed: 1868865]

Finkelman FD, Shea-Donohue T, Morris SC, Gildea L, Strait R, Madden KB, Schopf L, Urban JF Jr. Interleukin-4- and interleukin-13-mediated host protection against intestinal nematode parasites. Immunol Rev. 2004; 201:139–155. [PubMed: 15361238]

Gause WC, Urban JF Jr, Stadecker MJ. The immune response to parasitic helminths: insights from murine models. Trends Immunol. 2003; 24:269–277. [PubMed: 12738422]

Gordon S. Alternative activation of macrophages. Nat Rev Immunol. 2003; 3:23–35. [PubMed: 12511873]

Grewal JS, Kaur S, Bhatti G, Ganguly NK, Mahajan RC, Malla N. Kinetics of humoral & cellular immune responses in experimental cysticercosis in pigs infected with Taenia solium. Indian J Med Res. 2000; 111:43–49. [PubMed: 10824466]

Harn DA, McDonald J, Atochina O, Da'dara AA. Modulation of host immune responses by helminth glycans. Immunol Rev. 2009; 230:247–257. [PubMed: 19594641]

Hesse M, Modolell M, La Flamme AC, Schito M, Fuentes JM, Cheever AW, Pearce EJ, Wynn TA. Differential regulation of nitric oxide synthase-2 and arginase-1 by type 1/type 2 cytokines in vivo: granulomatous pathology is shaped by the pattern of L-arginine metabolism. J Immunol. 2001; 167:6533–6544. [PubMed: 11714822]

Joshi AD, Raymond T, Coelho AL, Kunkel SL, Hogaboam CM. A systemic granulomatous response to Schistosoma mansoni eggs alters responsiveness of bone-marrow-derived macrophages to Toll-like receptor agonists. J Leukoc Biol. 2008; 83:314–324. [PubMed: 18029396]

Keegan AD, Johnston JA, Tortolani PJ, McReynolds LJ, Kinzer C, O'Shea JJ, Paul WE. Similarities and differences in signal transduction by interleukin 4 and interleukin 13: analysis of Janus kinase activation. Proc Natl Acad Sci U S A. 1995; 92:7681–7685. [PubMed: 7544000]

Kigerl KA, Gensel JC, Ankeny DP, Alexander JK, Donnelly DJ, Popovich PG. Identification of two distinct macrophage subsets with divergent effects causing either neurotoxicity or regeneration in the injured mouse spinal cord. J Neurosci. 2009; 29:13435–13444. [PubMed: 19864556]

Kreider T, Anthony RM, Urban JF Jr, Gause WC. Alternatively activated macrophages in helminth infections. Curr Opin Immunol. 2007; 19:448–453. [PubMed: 17702561]

Lehnardt S, Henneke P, Lien E, Kasper DL, Volpe JJ, Bechmann I, Nitsch R, Weber JR, Golenbock DT, Vartanian T. A mechanism for neurodegeneration induced by group B streptococci through activation of the TLR2/MyD88 pathway in microglia. J Immunol. 2006; 177:583–592. [PubMed: 16785556]

Leonard WJ, O'Shea JJ. Jaks and STATs: biological implications. Annu Rev Immunol. 1998; 16:293–322. [PubMed: 9597132]

Lumeng CN, Bodzin JL, Saltiel AR. Obesity induces a phenotypic switch in adipose tissue macrophage polarization. J Clin Invest. 2007; 117:175–184. [PubMed: 17200717]

Mantovani A, Sica A, Locati M. Macrophage polarization comes of age. Immunity. 2005; 23:344–346. [PubMed: 16226499]

Mantovani A, Sica A, Locati M. New vistas on macrophage differentiation and activation. Eur J Immunol. 2007; 37:14–16. [PubMed: 17183610]

Mantovani A, Sica A, Sozzani S, Allavena P, Vecchi A, Locati M. The chemokine system in diverse forms of macrophage activation and polarization. Trends Immunol. 2004; 25:677–686. [PubMed: 15530839]

Martin P, Leibovich SJ. Inflammatory cells during wound repair: the good, the bad and the ugly. Trends Cell Biol. 2005; 15:599–607. [PubMed: 16202600]

Martinez FO, Gordon S, Locati M, Mantovani A. Transcriptional profiling of the human monocyte-to-macrophage differentiation and polarization: new molecules and patterns of gene expression. J Immunol. 2006; 177:7303–7311. [PubMed: 17082649]

Martinez FO, Helming L, Gordon S. Alternative activation of macrophages: an immunologic functional perspective. Annu Rev Immunol. 2009; 27:451–483. [PubMed: 19105661]

Martinez FO, Sica A, Mantovani A, Locati M. Macrophage activation and polarization. Front Biosci. 2008; 13:453–461. [PubMed: 17981560]

Mishra BB, Gundra UM, Teale JM. Expression and distribution of Toll-like receptors 11-13 in the brain during murine neurocysticercosis. J Neuroinflammation. 2008; 5:53. [PubMed: 19077284]

Mishra BB, Gundra UM, Wong K, Teale JM. MyD88-deficient mice exhibit decreased parasite induced immune responses but reduced disease severity in a murine model of neurocysticercosis. Infect Immun. 2009

Mishra BB, Mishra PK, Teale JM. Expression and distribution of Toll-like receptors in the brain during murine neurocysticercosis. J Neuroimmunol. 2006; 181:46–56. [PubMed: 17011049]

Modolell M, Corraliza IM, Link F, Soler G, Eichmann K. Reciprocal regulation of the nitric oxide synthase/arginase balance in mouse bone marrowderived macrophages by TH1 and TH2 cytokines. Eur J Immunol. 1995; 25:1101–1104. [PubMed: 7537672]

Mosser DM. The many faces of macrophage activation. J Leukoc Biol. 2003; 73:209–212. [PubMed: 12554797]

Mosser DM, Edwards JP. Exploring the full spectrum of macrophage activation. Nat Rev Immunol. 2008; 8:958–969. [PubMed: 19029990]

Moy FJ, Diblasio E, Wilhelm J, Powers R. Solution structure of human IL-13 and implication for receptor binding. J Mol Biol. 2001; 310:219–230. [PubMed: 11419948]

Munder M, Eichmann K, Modolell M. Alternative metabolic states in murine macrophages reflected by the nitric oxide synthase/arginase balance: competitive regulation by CD4+ T cells correlates with Th1/Th2 phenotype. J Immunol. 1998; 160:5347–5354. [PubMed: 9605134]

Nash TE, Singh G, White AC, Rajshekhar V, Loeb JA, Proano JV, Takayanagui OM, Gonzalez AE, Butman JA, DeGiorgio C, Del Brutto OH, Delgado-Escueta A, Evans CA, Gilman RH, Martinez SM, Medina MT, Pretell EJ, Teale J, Garcia HH. Treatment of neurocysticercosis: current status and future research needs. Neurology. 2006; 67:1120–1127. [PubMed: 17030744]

Nathan C, Shiloh MU. Reactive oxygen and nitrogen intermediates in the relationship between mammalian hosts and microbial pathogens. Proc Natl Acad Sci U S A. 2000; 97:8841–8848. [PubMed: 10922044]

Nauta AJ, Raaschou-Jensen N, Roos A, Daha MR, Madsen HO, Borrias-Essers MC, Ryder LP, Koch C, Garred P. Mannose-binding lectin engagement with late apoptotic and necrotic cells. Eur J Immunol. 2003; 33:2853–2863. [PubMed: 14515269]

Nelms K, Keegan AD, Zamorano J, Ryan JJ, Paul WE. The IL-4 receptor: signaling mechanisms and biologic functions. Annu Rev Immunol. 1999; 17:701–738. [PubMed: 10358772]

Noel W, Raes G, Hassanzadeh Ghassabeh G, De Baetselier P, Beschin A. Alternatively activated macrophages during parasite infections. Trends Parasitol. 2004; 20:126–133. [PubMed: 15036034]

O'Connell AE, Kerepesi LA, Vandergrift GL, Herbert DR, TJ VANW, Hooper DC, Pearce EJ, Abraham D. IL-4(-/-) mice with lethal Mesocestoides corti infections--reduced Th2 cytokines and alternatively activated macrophages. Parasite Immunol. 2009; 31:741–749. [PubMed: 19891612]

Obiri NI, Debinski W, Leonard WJ, Puri RK. Receptor for interleukin 13. Interaction with interleukin 4 by a mechanism that does not involve the common gamma chain shared by receptors for interleukins 2, 4, 7, 9, and 15. J Biol Chem. 1995; 270:8797–8804. [PubMed: 7721786]

Obiri NI, Murata T, Debinski W, Puri RK. Modulation of interleukin (IL)-13 binding and signaling by the gammac chain of the IL-2 receptor. J Biol Chem. 1997; 272:20251–20258. [PubMed: 9242704]

Pauleau AL, Rutschman R, Lang R, Pernis A, Watowich SS, Murray PJ. Enhancer-mediated control of macrophage-specific arginase I expression. J Immunol. 2004; 172:7565–7573. [PubMed: 15187136]

Pesce JT, Ramalingam TR, Mentink-Kane MM, Wilson MS, El Kasmi KC, Smith AM, Thompson RW, Cheever AW, Murray PJ, Wynn TA. Arginase-1-expressing macrophages suppress Th2 cytokine-driven inflammation and fibrosis. PLoS Pathog. 2009a; 5:e1000371. [PubMed: 19360123]

Pesce JT, Ramalingam TR, Wilson MS, Mentink-Kane MM, Thompson RW, Cheever AW, Urban JF Jr, Wynn TA. Retnla (relmalpha/fizz1) suppresses helminth-induced Th2-type immunity. PLoS Pathog. 2009b; 5:e1000393. [PubMed: 19381262]

Raes G, Brys L, Dahal BK, Brandt J, Grooten J, Brombacher F, Vanham G, Noel W, Bogaert P, Boonefaes T, Kindt A, Van den Bergh R, Leenen PJ, De Baetselier P, Ghassabeh GH. Macrophage galactose-type C-type lectins as novel markers for alternatively activated macrophages elicited by parasitic infections and allergic airway inflammation. J Leukoc Biol. 2005; 77:321–327. [PubMed: 15591125]

Reece JJ, Siracusa MC, Scott AL. Innate immune responses to lung-stage helminth infection induce alternatively activated alveolar macrophages. Infect Immun. 2006; 74:4970–4981. [PubMed: 16926388]

Restrepo BI, Alvarez JI, Castano JA, Arias LF, Restrepo M, Trujillo J, Colegial CH, Teale JM. Brain granulomas in neurocysticercosis patients are associated with a Th1 and Th2 profile. Infect Immun. 2001; 69:4554–4560. [PubMed: 11401999]

Restrepo BI, Llaguno P, Sandoval MA, Enciso JA, Teale JM. Analysis of immune lesions in neurocysticercosis patients: central nervous system response to helminth appears Th1-like instead of Th2. J Neuroimmunol. 1998; 89:64–72. [PubMed: 9726827]

Reyes JL, Terrazas LI. The divergent roles of alternatively activated macrophages in helminthic infections. Parasite Immunol. 2007; 29:609–619. [PubMed: 18042168]

Saba K, Denda-Nagai K, Irimura T. A C-type lectin MGL1/CD301a plays an anti-inflammatory role in murine experimental colitis. Am J Pathol. 2009; 174:144–152. [PubMed: 19095961]

Sato K, Imai Y, Higashi N, Kumamoto Y, Onami TM, Hedrick SM, Irimura T. Lack of antigen-specific tissue remodeling in mice deficient in the macrophage galactose-type calcium-type lectin 1/CD301a. Blood. 2005; 106:207–215. [PubMed: 15784728]

Sciutto E, Chavarria A, Fragoso G, Fleury A, Larralde C. The immune response in Taenia solium cysticercosis: protection and injury. Parasite Immunol. 2007; 29:621–636. [PubMed: 18042169]

Stein M, Keshav S, Harris N, Gordon S. Interleukin 4 potently enhances murine macrophage mannose receptor activity: a marker of alternative immunologic macrophage activation. J Exp Med. 1992; 176:287–292. [PubMed: 1613462]

Terrazas LI. The complex role of pro- and anti-inflammatory cytokines in cysticercosis: immunological lessons from experimental and natural hosts. Curr Top Med Chem. 2008; 8:383–392. [PubMed: 18393901]

Umemura N, Saio M, Suwa T, Kitoh Y, Bai J, Nonaka K, Ouyang GF, Okada M, Balazs M, Adany R, Shibata T, Takami T. Tumor-infiltrating myeloid-derived suppressor cells are pleiotropic-inflamed monocytes/macrophages that bear M1- and M2-type characteristics. J Leukoc Biol. 2008; 83:1136–1144. [PubMed: 18285406]

Urban JF Jr, Noben-Trauth N, Donaldson DD, Madden KB, Morris SC, Collins M, Finkelman FD. IL-13, IL-4Ralpha, and Stat6 are required for the expulsion of the gastrointestinal nematode parasite Nippostrongylus brasiliensis. Immunity. 1998; 8:255–264. [PubMed: 9492006]

van Riet E, Hartgers FC, Yazdanbakhsh M. Chronic helminth infections induce immunomodulation: consequences and mechanisms. Immunobiology. 2007; 212:475–490. [PubMed: 17544832]

Voehringer D, van Rooijen N, Locksley RM. Eosinophils develop in distinct stages and are recruited to peripheral sites by alternatively activated macrophages. J Leukoc Biol. 2007; 81:1434–1444. [PubMed: 17339609]

White AC Jr. Neurocysticercosis: updates on epidemiology, pathogenesis, diagnosis, and management. Annu Rev Med. 2000; 51:187–206. [PubMed: 10774460]

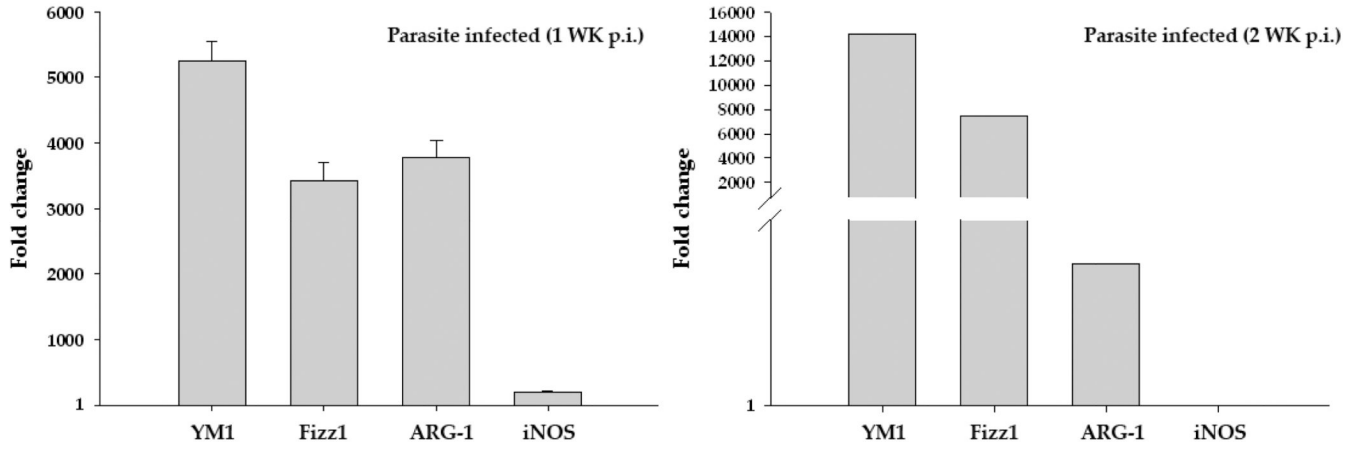

Figure 1. *M. corti* infection results in increased RNA expression of AAM markers

Total RNA was isolated from infected and vehicle control mice brains at 1 wk and 2 wk p.i. using Trizol reagent. Isolated RNA was reversed transcribed to cDNA by using random primers. The mRNA transcript levels of YM1, Fizz1, ARG-1, and iNOS as well as housekeeping genes 18S, beta actin and GAPDH in these samples were measured by Real Time PCR analysis using SYBR green as the detection dye. Expression of each specific gene in infected samples was determined as fold change over that in control samples as calculated by using the formula $2^{-(\Delta\Delta Ct)}$ (after normalizing with housekeeping genes). The data represent the mean ± SEM of three independent experiments at 1wk p.i. and mean of two independent experiments at 2wk p.i.

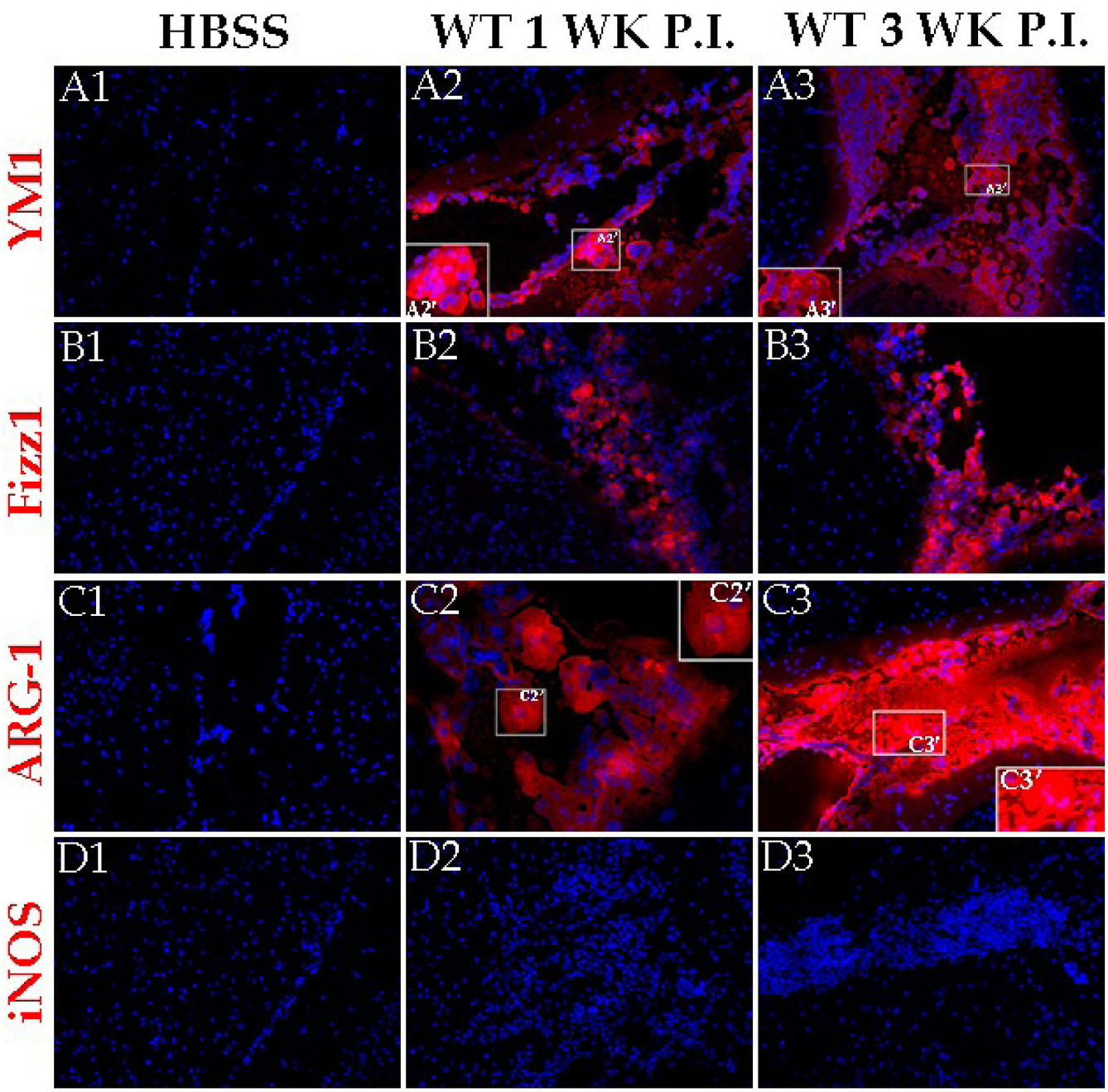

Figure 2. AAM related proteins are abundantly expressed in the *M. corti* infected brains

C57BL/6 mice were infected i.c. with *M. corti* and sacrificed at various times p.i. Brain cryosections were analyzed for expression of YM1, Fizz1, ARG-1, and iNOS using fluorochrome (red) conjugated antibodies. Nuclei (blue) were stained with 4'6' diamidino-2-phenylindol-dilactate (DAPI). Mock infected control stained with YM1 (A1), Fizz1 (B1) or ARG-1 (C1) specific antibody. Increased expression of YM1 was detected in leukocytes present in the meninges at 1 wk p.i. (A2) and 3 wk p.i. (A3). The insert A2' and A3' represents 2X magnification of a selected area of A2 and A3 respectively to better illustrate extracellular localization of YM1. Increased expression of Fizz1 detected in leukocytes present in the meninges at 1 wk p.i. (B2) and 3 wk p.i. (B3). Increased expression of ARG-1

detected in leukocytes present in the meninges at 1 wk p.i. (C2) and 3 wk p.i. (C3). The insert C2' and C3' represents 2X magnification of a selected area of C2 and C3 respectively to better illustrate extracellular localization of ARG-1. iNOS staining was undetected in the CNS of mock infected (D1) as well as in infected brains at 1 wk (D2) and 3 wk (D3) p.i. Results are from one representative experiment of five independent experiments; Magnification X 200.

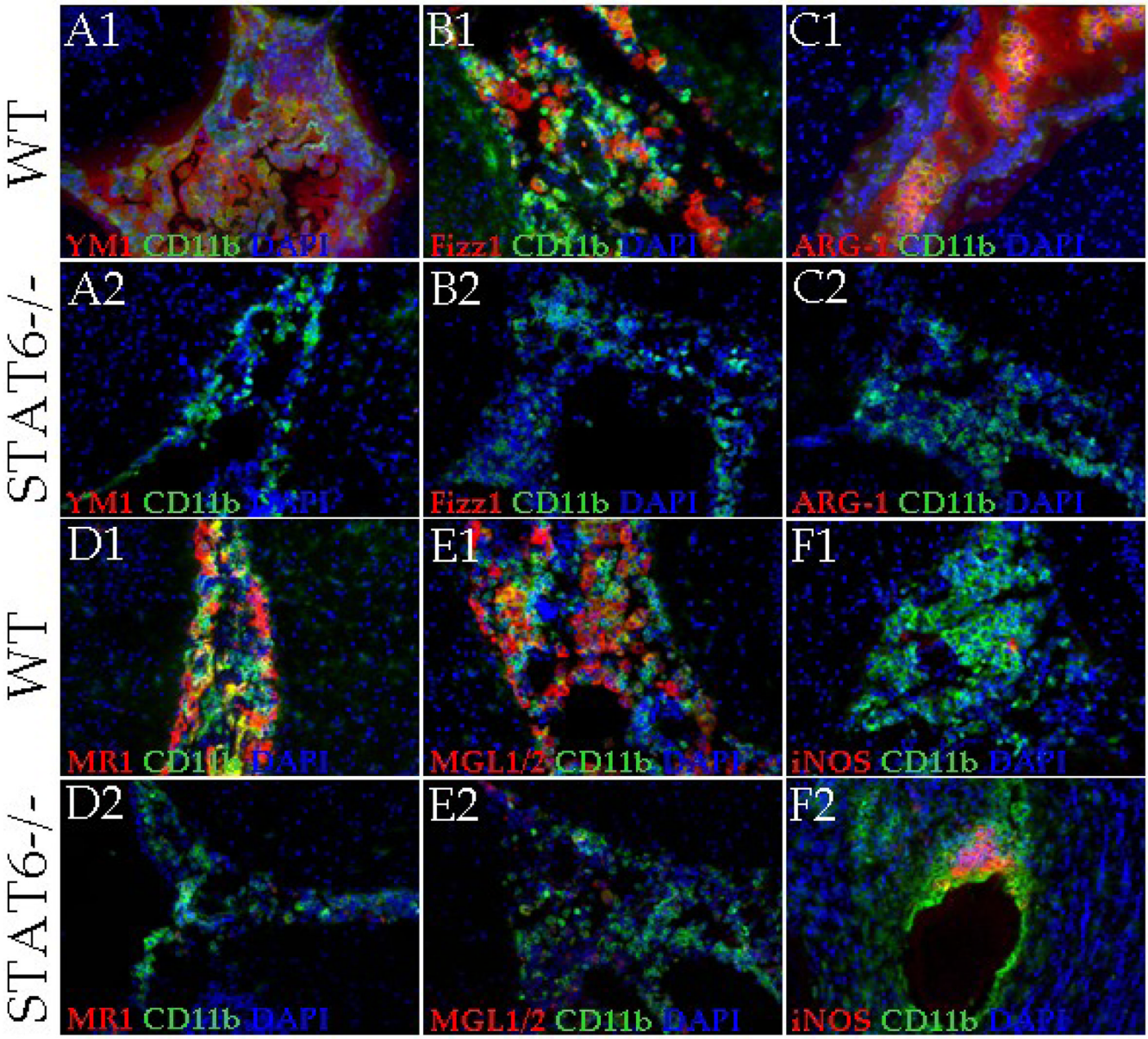

Figure 3. STAT6$^{-/-}$ mice present reduced expression of AAM related molecules

IF staining was performed on frozen sections of mock control and parasite-infected brains of WT or STAT6$^{-/-}$ mice at 2 wk p.i. YM1, Fizz1, ARG-1, MR1, MGL1/2 and iNOS expression was visualized in red (Rhodamine RXX), macrophages (CD11b+) were visualized in green (Alexa Fluor 488) and nucleic acid (blue) were stained with DAPI. Parasite-infected WT mice brains displayed large number of CD11b+ cells stained positive for YM1 (A1), Fizz1 (B1), ARG-1 (C1), MR1 (D1), and MGL1/2 (E1) at 2 wk p.i., yellow/orange. In contrast, staining for these AAM associated markers YM1 (A2), Fizz1 (B2), ARG-1 (C2), MR1 (D2), and MGL1/2 (E2) was undetected/barely detected in the macrophages accumulated in the CNS of STAT6$^{-/-}$ NCC mice. (F1) Staining for CAM associated marker iNOS was barely detected in WT NCC brain at 2 wk p.i. (F2) Increased number of accumulated macrophages was detected positive for iNOS in STAT6$^{-/-}$ NCC brains at 2 wk p.i., co-localization yellow/orange. Results are from one representative experiment of three independent experiments; Magnification X 200.

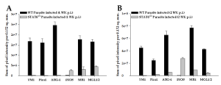

Figure 4. Quantification of brain level protein expression of YM1, Fizz1, ARG-1, and iNOS in WT and STAT6$^{-/-}$ mice

IF staining was performed on frozen sections of mock infected and parasite-infected brains of WT and STAT6$^{-/-}$ mice at 2 wk p.i. YM1, Fizz1, ARG-1, and iNOS expression was visualized in red (Rhodamine RXX). The relative levels of these molecules in mock and *M. corti* infected STAT6$^{-/-}$ or WT animals were calculated as described in experimental procedures. The modulated expression of these immune mediators in the CNS of parasite-infected STAT6$^{-/-}$ mice is statistically significant ($p<0.001$). Results are from three independent experiments.

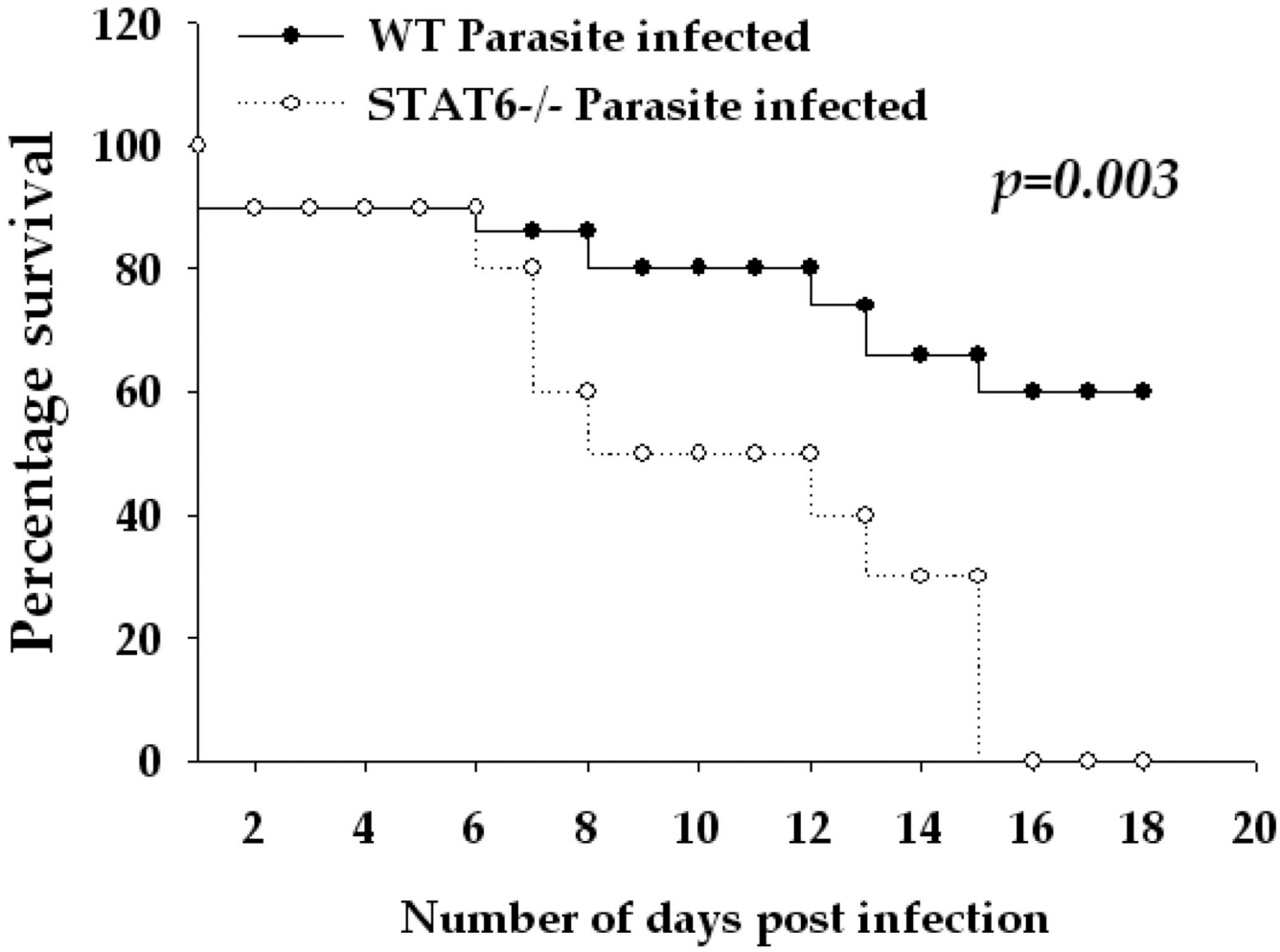

Figure 5. STAT6$^{-/-}$ mice display increased susceptibility during murine NCC

Fifteen mice of WT (C57BL/6) and ten mice of STAT6$^{-/-}$ were i.c. infected with ~40 *M. corti* metacestodes and assessed daily for disease severity. The increased susceptibility of STAT6$^{-/-}$ mice as compared to the WT mice is statistically significant as determined by Kaplan-Meier survival curve statistical analysis ($p<0.005$).

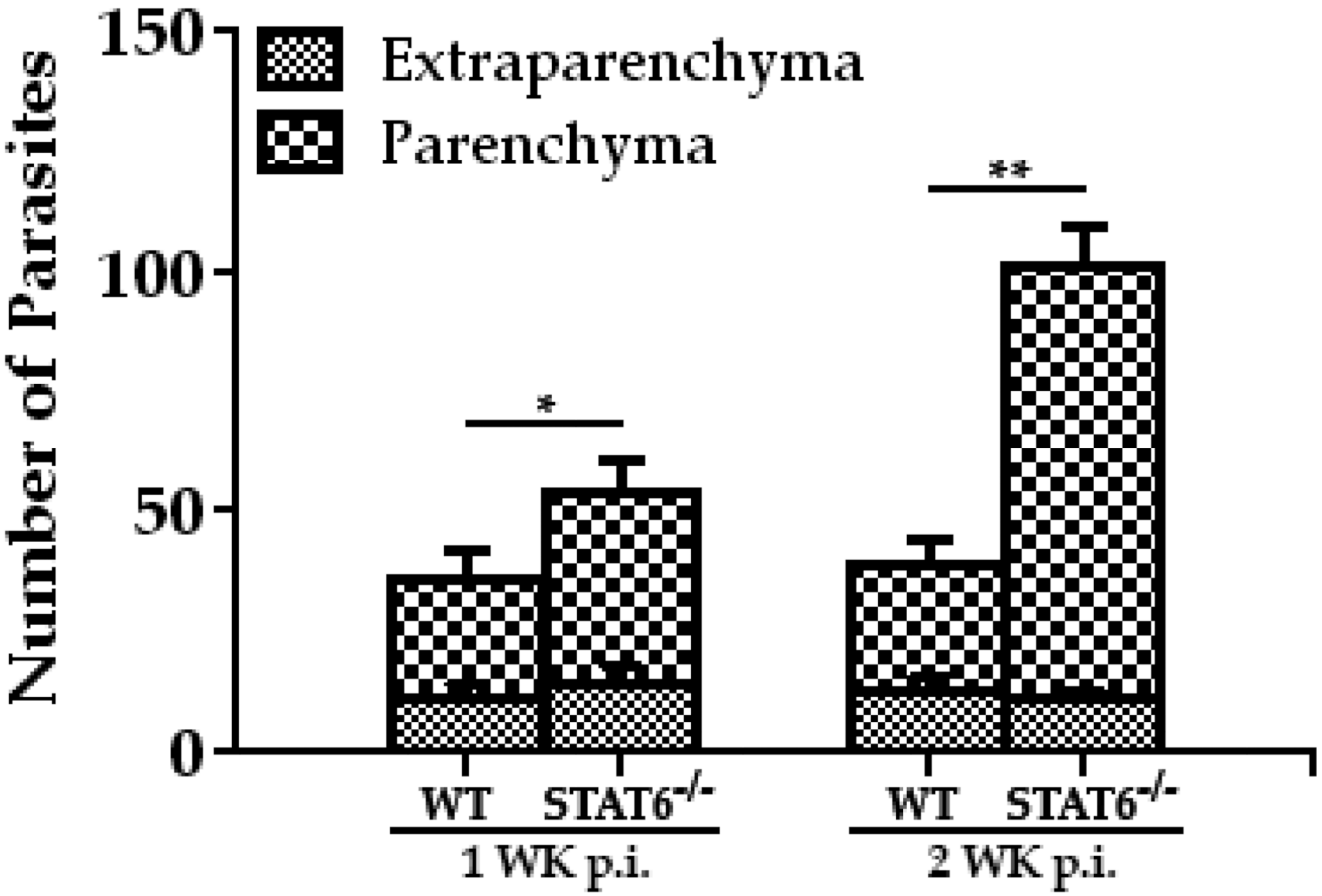

Figure 6. CNS infection with *M. corti* in STAT6$^{-/-}$ mice resulted in increased parasite burden in CNS

The WT (C57BL/6) and STAT6$^{-/-}$ were i.c. infected with ~40 *M. corti* metacestodes. After 1 wk and 2 wk of infection, mice were sacrificed and the location and number of parasites was enumerated in parenchymal and extraparenchymal regions by microscopic examination of serial H&E-stained brain sections. The significant differences in parasite numbers in *M. corti* infected STAT6$^{-/-}$ as compared with the infected WT animals are denoted by asterisks (*, $p<0.05$; **, $p<0.005$). Results are from three independent experiments.

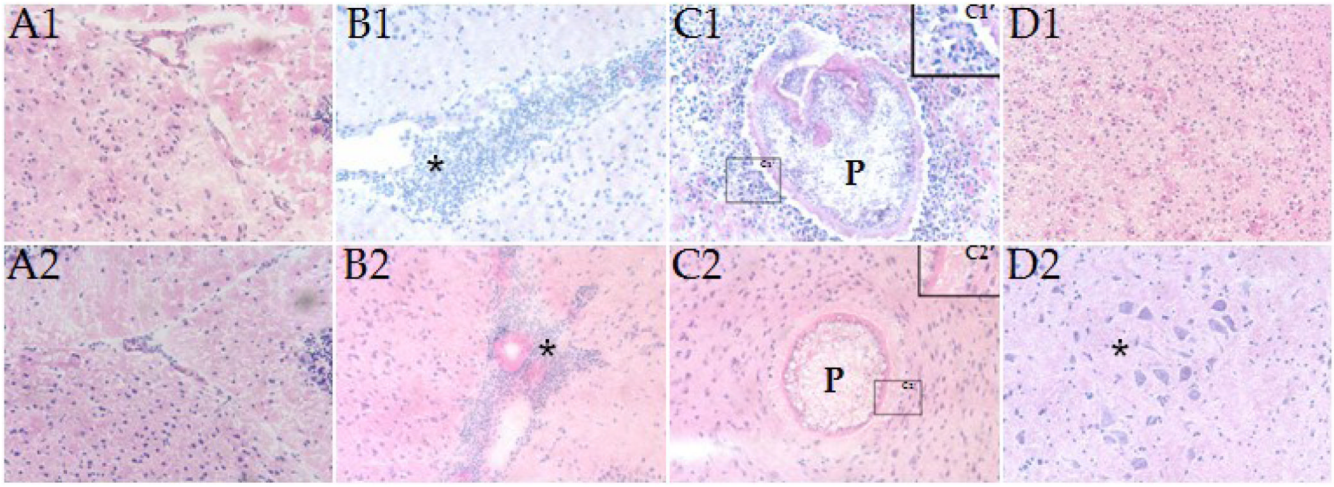

Figure 7. Brain pathology associated with *M. corti* infection in WT and STAT6$^{-/-}$ mice

H&E staining of brain cryosections showing (A1) normal parenchymal tissue in a HBSS-inoculated WT mouse. (A2) Normal parenchymal tissue in a HBSS-inoculated STAT6$^{-/-}$ mouse. (B1) Internal meninges area of the brain in a WT mouse at 2 wk p.i. associated with massive infiltrating immune cells (*). (B2) Internal meninges area of the brain in a STAT6$^{-/-}$ mouse at 2 wk p.i. associated with large number of infiltrating immune cells. (C1) Parenchymal parasite in a WT mouse at 2 wk p.i. associated with infiltrating immune cells; P- Parasite; C1') The boxed area in C1 was magnified (4X) to show the infiltrating immune cells in WT mice. (C2) Parenchymal parasite in a STAT6$^{-/-}$ mouse at 2 wk p.i. associated with lower numbers to absence of infiltrating immune cells; P-Parasite. (C2') The boxed area in C2 was magnified (4X) to show absence of infiltrating leukocytes around the parenchymal parasites in the STAT6$^{-/-}$ NCC mice brains. (D1) Parenchyma of a WT mouse at 1 wk p.i. exhibiting absence of microglial nodule formation. (D2) Parenchyma of a STAT6$^{-/-}$ mouse at 1 wk p.i. exhibiting microglial nodule formation (*). Results are from one representative experiment of three independent experiments.